Transport Simulation and Di ractive Event Reconstruction at the LHC

R. Staszewski[a] and J. Chwastowski[b a]

[a] Institute of Nuclear Physics PAN, ul. Radzikowskiego 152,
31-342 Krakow, Poland.

[b] Chair of Teleinformatics,
Faculty of Physics, Mathematics and Applied Computer Science,
Cracow University of Technology,
ul. Warszawska 24, 31-115 Krakow, Poland.

The measurement of di ractively scattered protons in the ATLAS Forward Physics detector system placed 220 m away from the ATLAS interaction point is studied. A parameterisation of the scattered proton transport through the LHC magnet lattice is presented. The proton energy unfolding and its impact on the centrally produced scalar particle mass resolution are discussed.

1. Introduction

Di ractive dissociation is one of the processes that can be studied at the LHC. Di ractive physics is strong interaction physics involving no exchange of quantum numbers other than those of the vacuum. In experiment this leads to an obvious triggering scheme relying on the rapidity gap method. However, one has to keep in mind that the gap has a certain survival probability that depends on the interaction type and the centre of mass energy. In addition, also the di ractively scattered protons can be tagged. Usually, the protons scatter at small angles and in the collider environment they stay in the beam pipe and travel through the magnet lattice of the machine. A possible way to measure parameters of the di ractively scattered proton trajectory is to use detectors placed inside the beam pipe, for example by means of a roman pot station or a movable beam pipe technique. The ATLAS Collaboration plans to have proton tagging stations placed symmetrically with respect to the Interaction Point (IP) at the distances of 220 m and 420 m (AFP220 and AFP420) and 240 m (ALFA). The ALFA (Absolute Luminosity For Atlas) [1] stations at 240 m will be devoted to the absolute luminosity measurement of the LHC at the ATLAS IP. This measurement will rely on the detection of the elastically scattered protons. The AFP (Atlas Forward Physics) [2] stations will be used for di ractive and physics.

This work was supported in part by the ECO-NET Programme: \To Study the Forward Physics at the LHC and the Search for the Higgs Boson in Di raction" and Polish grants PBS-CERN/85/2006 and 319/N-CERN/2008/09/0

2. Experimental Environment

Below, only the aspects concerning the AFP220 detectors are discussed. In the measurement, the machine magnets play the role of magnetic spectrometer. Therefore, two detector stations are to be placed around 220 m, namely one at 216 and one at 224 m. Each station will be equipped with position sensitive and triggering detectors, horizontally inserted into the LHC beam pipe. The position sensitive detectors will consist of 10 layers of the silicon 3D detectors [3] to measure the scattered proton trajectory. The position measurement resolutions are assumed to be $\sigma_x = 10$ μm and $\sigma_y = 40$ μm in the horizontal and vertical direction, respectively. This will allow the measurement of the particle trajectory position and direction. Additionally, the stations will contain very fast timing detectors with picosecond resolution. They will measure the scattered proton time of flight and indicate the interaction vertex longitudinal coordinate, z, with resolution of the order of several millimeters. In the following calculations, a reference frame with the x–axis pointing towards the accelerator centre, the y–axis pointing upwards and the z–axis along one of the beams was used.

The scattered proton can be described at the interaction point in several equivalent ways, each useful in a different case: (p_x, p_y, p_z), (E, x_0', y_0'), or (E, p_T),

$$E = \sqrt{m^2 + p^2} \qquad x_0' = \frac{p_x}{p_z} \qquad y_0' = \frac{p_y}{p_z}$$

where E and m are the proton energy and mass, $p = (p_x, p_y, p_z)$ is the proton momentum and $p_T = (p_x, p_y)$ denotes the proton transverse momentum. Useful variables are the proton energy loss $\Delta E = E_0 - E$ (E_0 is the incident beam energy), the reduced proton energy loss, $\xi = \Delta E / E_0$, and the four-momentum transfer between the incident and scattered proton, t.

There are several programs on the market calculating proton trajectories through the magnets. In the following the FPTrack program [4] was used. This program computes the positions of particles using the LHC optics files which describe the magnetic fields, positions and apertures of the LHC lattice. These files were produced with help of a principal beam transport program Mad-X [5] by the LHC optics group [6].

Table 1
The LHC beam and the crossing region parameters at the ATLAS IP.

Parameter	Beam	Crossing region
σ_{x_0}	16.6 μm	11.7 μm
σ_{y_0}	16.6 μm	11.7 μm
σ_{z_0}	75 mm	53 mm
$\sigma_{x_0'}$	30.2 μrad	
$\sigma_{y_0'}$	30.2 μrad	
σ_{E_0}	0.77 GeV	

The interaction vertex is described by its coordinates (x_0, y_0, z_0). These coordinates have Gaussian distributions with zero average values and dispersions: σ_{x_0}, σ_{y_0}, σ_{z_0}, respectively. In the simulation, the beam particle energy and its momentum direction were generated according to Gaussian distributions with appropriate means and the dispersions: σ_{E_0} for the energy and $\sigma_{x_0^0}$; $\sigma_{y_0^0}$ for the momentum in $(x;z)$ and $(y;z)$ planes, correspondingly. Values of these parameters for the nominal 7 TeV beam energy and standard LHC optics are listed in Table 1. The calculations were performed for both beams: beam 1 that performs the clockwise motion and beam 2 which does the counter clockwise rotation.

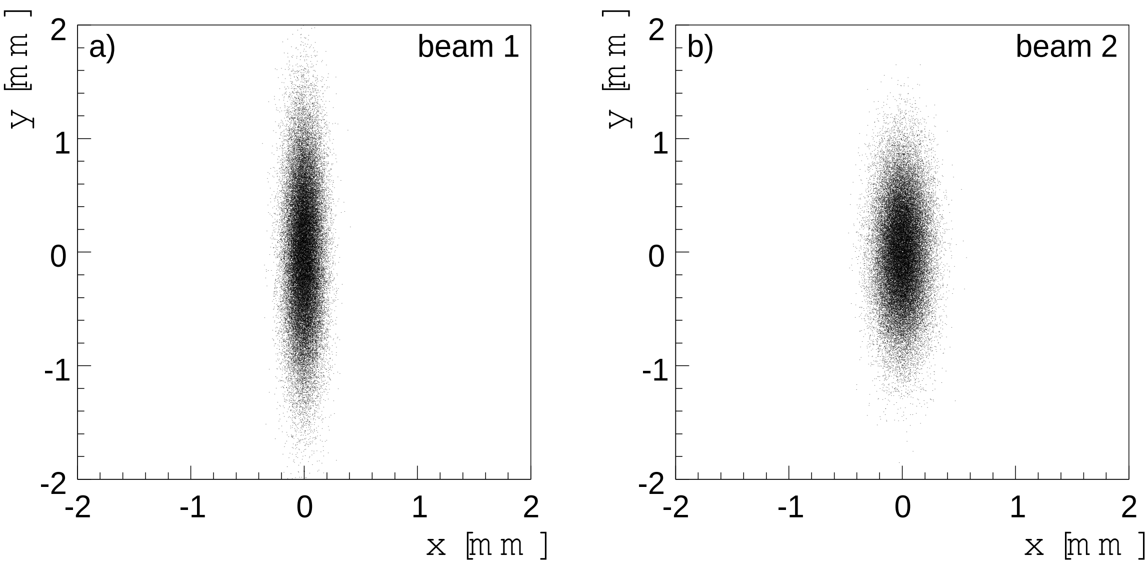

Figure 1. The LHC beam profiles at 216 meters from ATLAS IP for beam 1 (a) and beam 2 (b), for the 7 TeV LHC optics.

Figure 1 shows the LHC beam profiles in the (x,y) plane at 216 m away from the ATLAS IP obtained with the FTPtrack program for both beams and the 7 TeV LHC optics. As can be observed, the beams are much wider in the vertical direction than in the horizontal one.

Table 2 summarizes the beams spreads following from a two dimensional Gaussian fit to the beam profiles shown in Fig. 1. The (10 – 15) σ beam envelope gives a natural limit for the distance between the detector frame and the beam centre. In the horizontal direction this corresponds to about 1 – 2 millimeters. Obviously, this distance plays a crucial role for the diffractively scattered proton detection and hence, for the experimental apparatus acceptance.

It is important to see in which range of the energy, E, and the transverse momentum, $p_T = |p_T|$, the detector can measure protons. The geometric acceptance for fixed E and p_T values was defined as the ratio of the number of protons that crossed the detector to the total number of scattered protons with a given E and p_T. Only the effects of the beam pipe aperture and the distance between the detector and the beam centre were taken into account.

Figure 2 depicts the geometric acceptance as a function of E and p_T for beam 1 for the

Table 2
The LHC beam spreads from a Gaussian t to the beam pro les at 216 m.

Parameter	Beam 1	Beam 2
x_{216}	88 m	121 m
y_{216}	569 m	421 m

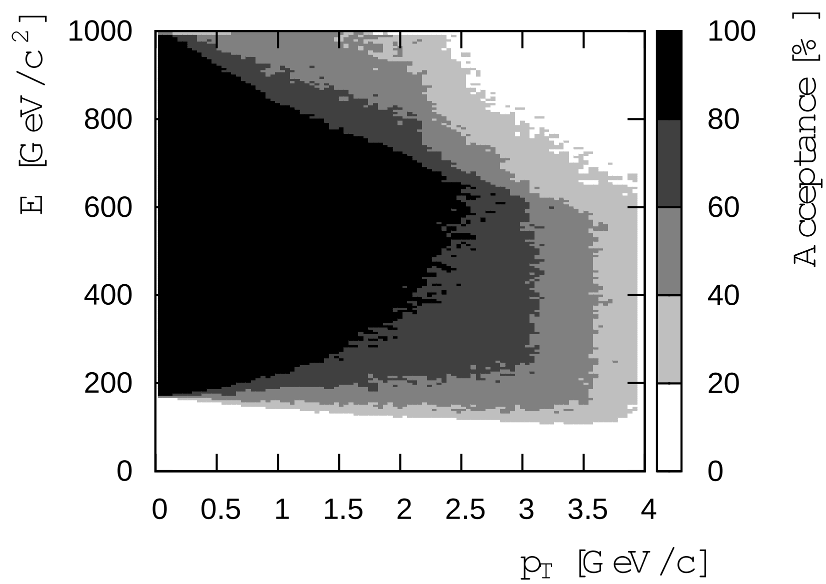

Figure 2. The geometrical acceptance of the detector placed in the LHC beam 1 at 216 m away from the IP as a function of the proton energy loss (E) and its transverse momentum p_T for a 3 mm distance between the beam centre and the detector active edge.

standard 7 TeV LHC optics. The acceptance is above 80% in the region limited by:

$$200 < E < 1000 \text{ [GeV]}; \; 0 < p_T < 2.5 \text{ [GeV/c]}$$

which corresponds to

$$0.03 < \; < 0.14; \quad 6.5 < t < 0 \text{ [GeV}^2\text{/c}^2\text{]}.$$

When the geometrical acceptance requirement is lowered to 60%, this results in a wider range of the accepted proton energies and transverse momenta. The range enlargement is seen (c.f. Fig. 2) for $200 < E < 600$ GeV and $p_T < 3$ GeV/c. This gives the limits:

$$0.03 < \; < 0.14; \quad 10 < t < 0 \text{ [GeV}^2\text{/c}^2\text{]}.$$

The presence of two detector stations on each side of the ATLAS detector allows the measurement of the proton trajectory elevation angles, x^0 and y^0, in the (x,z) and (y,z) planes, respectively. From the FPTrack calculations, it follows that the position and slope of the trajectory at the detector in one transverse direction is independent of those in the other direction, i.e. x and x' values do not depend on y_0 and y'_0 and vice versa. This is a reflection of a negligible role of the sextupole and higher order magnetic fields in the standard LHC optics between the ATLAS IP and the AFP220 stations.

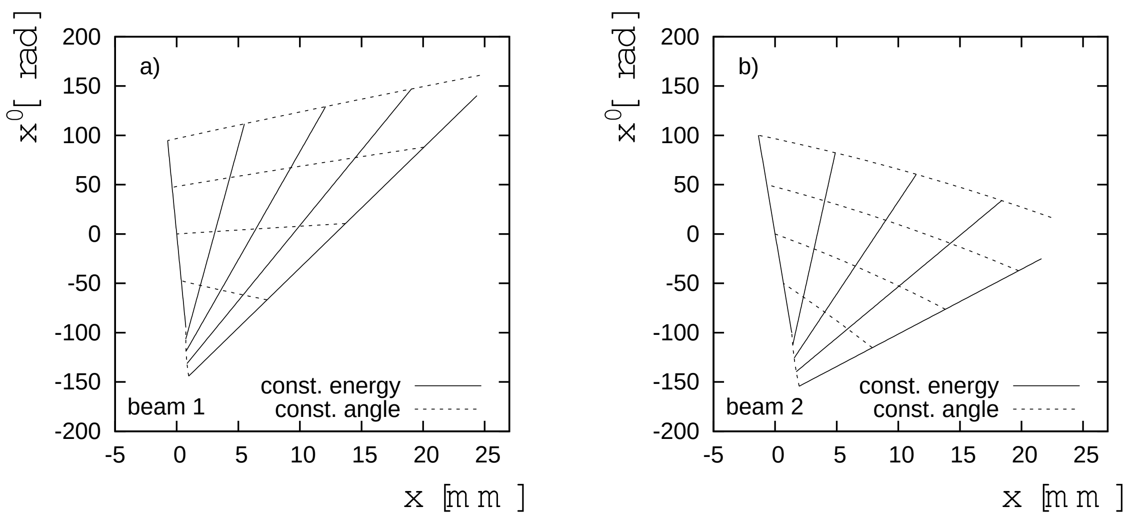

Figure 3. The x-direction chromaticity plots for the LHC beam 1 (a) and beam 2 (b) for the standard 7 TeV LHC optics. The lines of constant energy correspond to 7000, 6825, 6650, 6475, 6300 GeV from left to right, respectively. The angles were changes from −400 μrad to 400 μrad (from top to bottom).

To illustrate how the proton trajectory positions and slopes measured by the detectors depend on the proton energy and its trajectory slopes at the IP the chromaticity plots were prepared. The plots shown in Figure 3 were devised by plotting in the (x, x') plane the lines corresponding to the constant E and x'_0 at the IP.

The chromaticity plots indicate few things. Firstly, there is a non-negligible difference between both beams. Therefore, properties of both have to be studied. Secondly, the grids created by the energy and angle iso-lines do not fold. Hence, it is possible to obtain the energy and the transverse momentum of a proton from the measurements of the proton trajectory in both stations. In particular, assuming a fixed interaction vertex position (no smearing) the energy of a proton at the IP can be deducted solely from the measured x and x' values.

3. Transport Parameterisation

In order to unfold the proton energy from the detector measurements a parameterisation of the FPTrack transport calculations was prepared. The aim was to describe the FPTrack results analytically. It was requested that:

- the parameterisation has a simple functional form,
- the parameterisation precision has an accuracy which is better than the assumed detector spatial resolutions.

To find the parameterisation form, events uniformly distributed over the $(E; x_0^0; y_0^0; x_0; y_0; z_0)$ space were generated. Subsequently, these events were used in the FPTrack transport calculations. The transport results were the input data to the parameterisation search procedure. It was found that the following parameterisation fulfill the requirements outlined above well:

$$= A \quad + \quad {}^0_0 B \quad + \quad {}_0 C \quad + \quad {}^0_0 z_0 D \quad + z_0 F \ ; \tag{1}$$

$$^0 = A_s \quad + \quad {}^0_0 B_s \quad + \quad {}_0 C_s \quad + \quad {}^0_0 z_0 D_s \quad + z_0 F_s \ ; \tag{2}$$

where $= \{x; y\}$, s denotes the slope either in x or y direction and all the capitalised symbols are polynomials of energy, i.e.:

$$A \quad = a^{(0)} + a^{(1)} E + a^{(2)} E^2 + a^{(3)} E^3 + a^{(4)} E^4 ; \tag{3}$$

$$C_s \quad = c_s^{(0)} + c_s^{(1)} E + c_s^{(2)} E^2 + c_s^{(3)} E^3 : \tag{4}$$

The values of all the coefficients were found by fitting the formulae to the FTP track calculations for simulated events.

The accuracy of the method was estimated by plotting the difference between the value given by the parameterisation and that given by the FPTrack calculation. The accuracy of the position parameterisation was found to be of the order of a micrometer which is 10 times less than the assumed detector resolution in the horizontal plane. The difference between FPTrack and the parameterisations for the trajectory angles was found to be limited to about 50 nanoradians. One has to remember that the average multiple Coulomb scattering angle was estimated to be about 500 nrad. An example of the parameterisation accuracy is presented in Fig. 4. In this figure the distributions of $y = y_{param} \quad y_{FPTrack}$ and $y^0 = y^0_{param} \quad y^0_{FPTrack}$ are shown for single diffractive events generated with PYTHIA [8]. The accuracy estimations for these quantities are displayed since they represent the worst precision cases. Nevertheless, the results are well confined within the ranges given by the detector resolutions. This confirms the parameterisation quality.

One should note that the procedure outlined above can be easily repeated. In particular, it can be applied to the files describing the actual LHC collision optics used for experimental runs.

4. Event Reconstruction

Since there is a correlation between the proton momentum and the measured position of the proton at the AFP220, the reconstruction of the proton properties at the interaction vertex from the measured coordinates of the proton trajectory at the AFP220 is possible.

A proton at the interaction vertex is described by six independent variables: E, x_0^0, y_0^0, x_0, y_0 and z_0. The detectors deliver two pairs of transverse coordinates separated in longitudinal direction by a fixed distance of about 8 meters. In general, the unfolding problem is an ill-stated one. In the present case it requests the inversion of the 6 to 4 mapping and its solution is only possible with help of additional assumptions. The

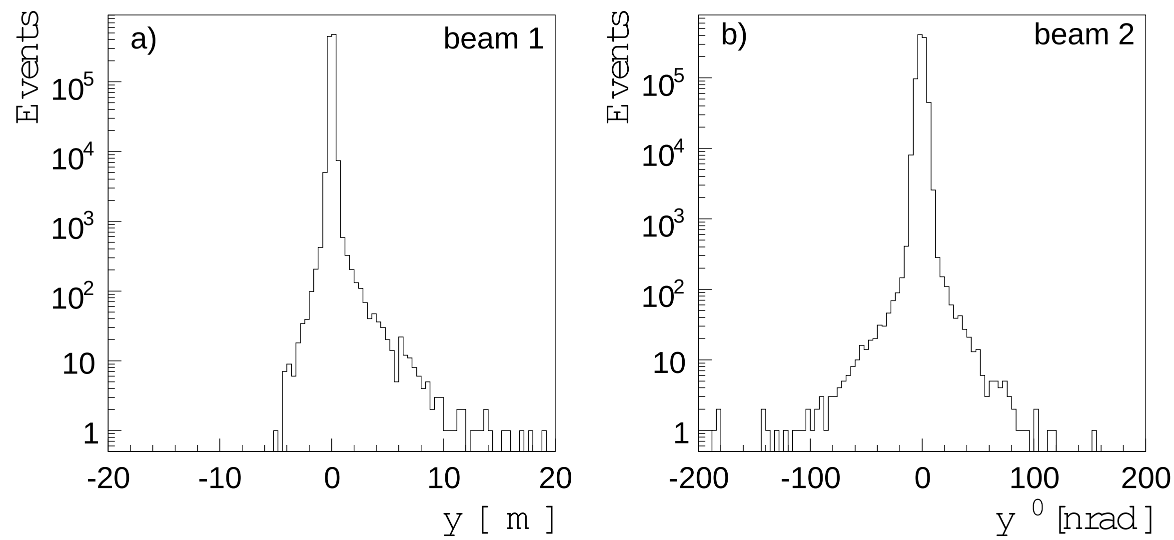

Figure 4. The parameterisation accuracy estimation examples (see text). Pictures show the uncertainty on the y (a) and y^0 (b) parameterisations of the beam 1 transport.

simplest one is the assumption of a fixed position of the interaction vertex. In the following the positions $x_0 = y_0 = 0$ and $z_0 = 0$ or $z_0 = 216\,\tau c$ were chosen, where τ is the proton time of flight.

To make the measurement simulation as close to reality as possible the detector effects were taken into account. Protons traversing the detector station undergo multiple Coulomb scattering in the frame and the detector materials. The simulation of the proton trajectory position measurement also takes into account the assumed detector resolutions. These effects may lead to a considerable change of the proton trajectory parameters (slopes and positions). Hadron interactions in the detector or its frame were neglected as they are not important for the present study.

A simple and fast method of the proton energy unfolding from the detector measurement is proposed. This method uses the assumption that the values actually measured are equal to those delivered by the parameterisation. This allows to calculate x_0^0 from eqs. (1) and (2). Since both equations are considered for the same particle, they should give equal values. Hence, after simple algebra one gets:

$$(x - A_x - F_x z_0 - x_0 C_x) \cdot (B_{sx} + z_0 D_{sx}) = \\ = (x^0 - A_{sx} - F_{sx} z_0 - x_0 C_{sx}) \cdot (B_x + z_0 D_x) \quad (5)$$

where all capitalised symbols are described by eqs. 3 and 4.

The solution of the above equation is equivalent to finding the zero of the function $f(E)$ given below:

$$f(E) = (x - A_x - F_x z_0 - x_0 C_x) \cdot (B_{sx} + z_0 D_{sx}) \\ - (x^0 - A_{sx} - F_{sx} z_0 - x_0 C_{sx}) \cdot (B_x + z_0 D_x). \quad (6)$$

It was observed that for obtained parameterisation and simulated events the function $f(E)$ has only one zero. Therefore, the equation

$$f(E) = 0$$

can be easily solved numerically using for example the bisection method [7].

The energy unfolding procedure was tested using the same PYTHIA generated data sample. The proton energy was reconstructed with the help of the different additional assumptions listed below:

- the “measured” trajectory coordinates were smeared according to the detector resolution,
- the interaction vertex transverse position was exactly known,
- the interaction vertex longitudinal position was exactly known.

The results are presented in Figure 5. The energy reconstruction resolution (the thick solid line) decreases from 9 GeV for 6000 GeV protons to about 3 GeV for 7000 GeV protons. It is dominated by the detector spatial resolution which influence, marked with the thick dashed line, decreases with proton energy from about 7 GeV to about 1 GeV within considered energy range. Also, the impact of the multiple Coulomb scattering (dotted line) gets smaller with increasing proton energy. Its contribution to the resolution is about 2.5 GeV at the maximum. For proton energies greater than 6800 GeV the uncertainty on the interaction vertex position in the transverse plane (the thick dash-dotted line)

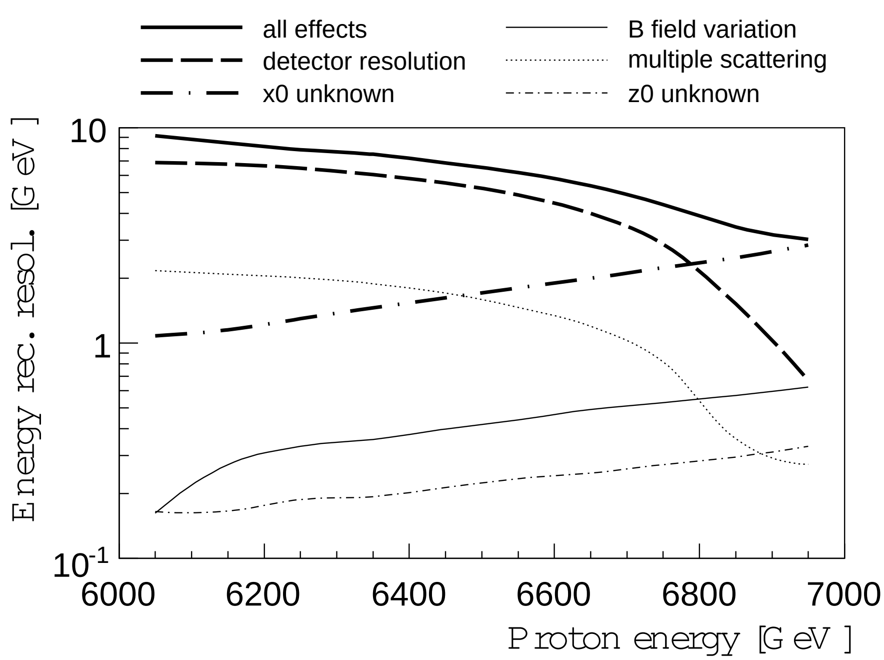

Figure 5. The proton energy reconstruction resolution for beam 1 as a function of its energy. The overall resolution is marked with the thick solid line, the influence of: the detector spatial resolution – the thick dashed line, the vertex position in the transverse plane – the thick dash-dotted line, the multiple Coulomb scattering – the dotted line, the vertex position along the beam axis – the dash-dotted line, the magnetic field variation – the solid line.

dominates the energy reconstruction resolution. The influence of the interaction vertex position along the longitudinal axis (the dash-dotted line) is small in the whole energy range discussed.

Since the scattered protons can traverse the whole beam pipe volume the influence of the possible imperfections of the magnetic fields was studied. The magnetic fields of the lattice were varied by ±1‰ of their nominal values. It should be pointed out that assumed variation is about a factor of 10 larger that the machine accepted and about 50 times larger than the measured values [9] of the higher multipoles at the reference radius of 17 mm away from the beam pipe centre. Variation of the magnetic field values gives a small contribution to the energy reconstruction resolution and for 6000 GeV protons it is about 0.3 GeV and increases to 0.7 GeV at 7000 GeV. This contribution is marked with the solid line in Fig. 5. The other effect of the variation of magnetic fields is the offset of the scattered proton reconstructed energy. This offset, on the absolute value, decreases linearly from about 1.3 GeV to approximately 0.1 GeV for proton energies between 6000 and 7000 GeV.

Another important experimental factor is the detector alignment. It is required that the detector stations will be able to measure the scattered proton trajectory elevation angles with precision of about 1 μrad. This implies a 10 μm precise alignment. It turned out that the 10 μm misalignment of the stations results an offset of the reconstructed proton energy. This offset has the largest value of about 5 GeV for protons of 6000 GeV energy and decreases to zero with proton energy increasing to 7000 GeV.

5. Central Exclusive Production (CEP)

The AFP detectors can be used to measure the exclusive central production of scalar $J^{PC} = 0^{++}$ particles (for example the Higgs boson or some supersymmetrical particles). The central production can be viewed as a two stage process. In a first step each of the incident protons emits a color singlet object. Subsequently, these objects interact with each other giving a centrally produced system. The incoming protons remain intact, traverse the magnetic lattice of the machine inside the beam pipe and can be detected in the AFP detectors. The centrally produced system decays into the ATLAS main detector. Hence, this gives a unique possibility to measure all the particles belonging to the final state (a completely exclusive event measurement).

Such events were simulated in a simplified way. In the generation the four momentum transfer, t, and the reduced proton energy loss, ξ, were distributed according to e^{-bt} with $b = 6\,\mathrm{GeV}^{-2}$ and ξ^{-1}, respectively. Later, the proton transport to the AFP220 detectors was simulated using the FPTrack calculations.

In Figure 6 the geometrical acceptance for different masses of the centrally produced system for various distances between the detector edge and the beam centre is shown. As expected, the geometrical acceptance strongly depends on this distance and for a realistic distance of 3 mm (marked with the dashed line in Figure 6) it varies between 0 and 30% for masses changing from 300 to 800 GeV.

Next, the mass of the centrally produced system was estimated using the detector measurements and the proton energy reconstruction described in section 4. For the Central Exclusive Production process the produced system mass determination from the reduced

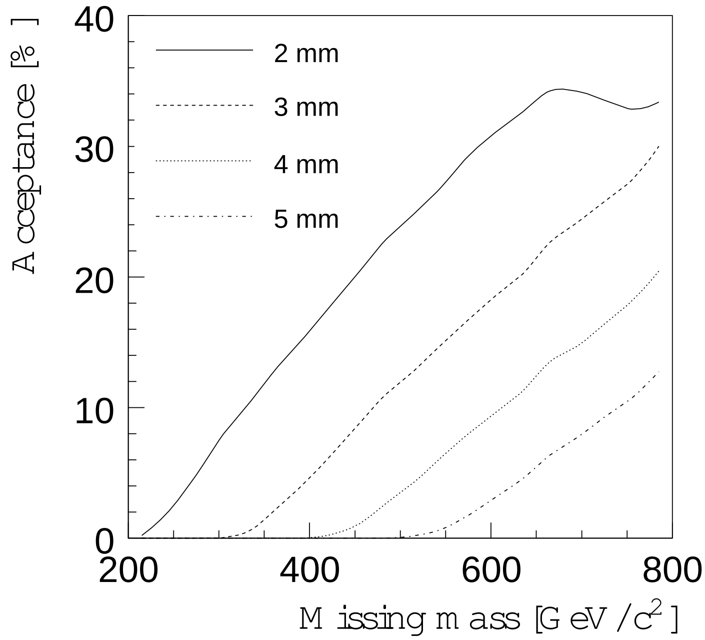

Figure 6. The geometrical acceptance of detectors at 216 m away from the ATLAS Interaction Point for Central Exclusive Production process as a function of the produced particle mass. The solid lines depicts the acceptance for active detector region at the 2 mm distance from the beam centre. The dashed, dotted and dash-dotted lines mark the acceptance curves for the 3, 4 and 5 mm distance, respectively.

energy losses of both protons, ξ_1 and ξ_2, is possible via [10]:

$$M_x = \sqrt{s\,\xi_1\,\xi_2};$$

where s is the centre of mass energy squared.

The mass reconstruction resolution as a function of the centrally produced system between 300 and 800 GeV is shown in Figure 7 for the 3 mm distance between the detector and the beam centre. The impact of several experimental factors is also depicted in this figure. The mass reconstruction resolution, after an initial jump at the acceptance edge, very slowly increases from 5 to 8 GeV with increasing value of the produced system mass. The influence of the multiple scattering, the beam energy variation and the proton direction angular spread is small and below 2 GeV. In fact, the resolution value is dominated by two factors. First one is the detector spatial resolution which gives the contribution ranging between 2 and 6 GeV and which dominates for masses above 500 GeV. The second one is the uncertainty on the x_0 coordinate of the interaction vertex, whose influence practically does not depend on the produced system mass and which is the most important factor for masses below 500 GeV. The field imperfections, estimated as described previously, have a small influence on the reconstructed mass resolution which is about 0.7 GeV at 300 GeV and saturates at the value of approximately 1 GeV at 500 GeV. Also, in this case the field variation resulted the mass offset which is about 1 GeV

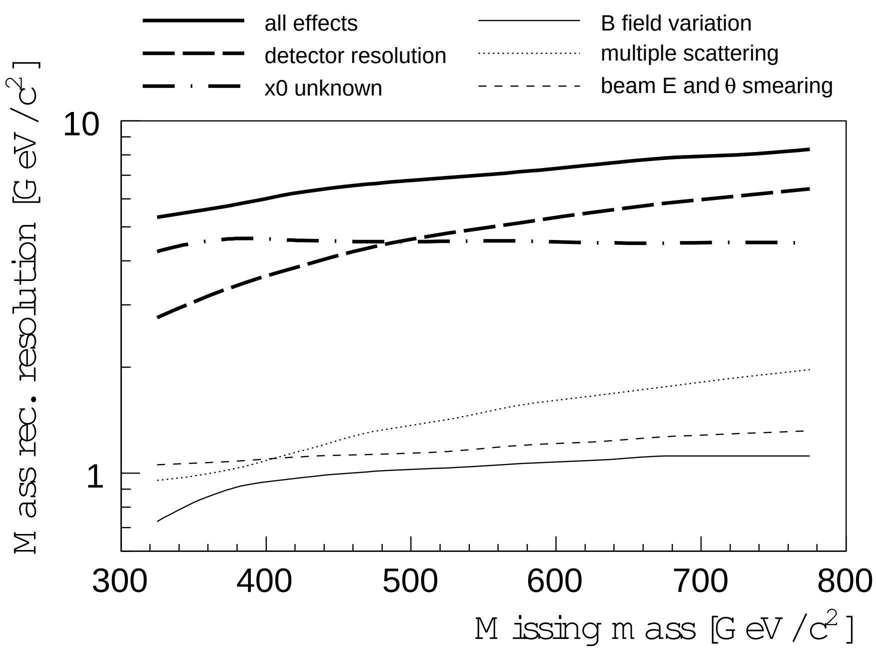

Figure 7. The centrally produced particle mass resolution determined with outgoing protons as a function of the particle mass. The overall mass reconstruction resolution is marked with the thick solid line, the influence of: the detector spatial resolution – the thick dashed line, the vertex position in the transverse plane – the thick dash-dotted line, the multiple Coulomb scattering – the dotted line, the magnetic field variation – the solid line, the beam energy and the proton direction angular spreads – the dashed line.

in the considered mass range. The impacts of the interaction vertex position and that of the detector misalignment, not shown in Figure 7, are small and below 0.5‰ of the produced mass value. The detector misalignment introduces the reconstructed mass shift which almost linearly increases with the produced mass value from about 2.5 GeV at 300 GeV to 6.5 GeV at 800 GeV.

6. Summary and Conclusions

A parameterisation of the proton transport through the magnet lattice of the LHC was devised. This parameterisation has a simple functional form and enables fast and easy calculations.

A proton energy unfolding procedure from the proton trajectory position measurements was prepared. This procedure allows the reconstruction of the scattered proton energy. The procedure was used to reconstruct the missing mass of the centrally produced scalar system. The missing mass reconstruction resolution weakly depends on the produced mass and reaches about 8 GeV at the mass value of 800 GeV.

The proton energy unfolding procedure can be used for the first level triggering of the apparatus at the LHC environment.

Acknowledgments

We are grateful to P. Bussey, A. Kupco, C. Royon, A. Siemko and J. Turnau for many discussions, useful remarks and help.

REFERENCES

1. ATLAS Collab., ATLAS Forward Detectors for Luminosity Measurement and Monitoring, Letter of Intent, CERN/LHCC-2004-010.
2. RP220 Collaboration, C. Royon for the collaboration, Proc. 15th Int. Workshop on Deep-Inelastic Scattering and Related Subjects (DIS2007), Munich, Germany, p. 759, M. G. Albrow et al., CERN-LHCC-2005-025, ATLAS Collab., AFP Letter of Intent, unpublished.
3. C. J. Kenney et al., Nucl. Instr. Meth. A 565 (2006) 272, M. Mathes et al., IEEE NS 55 (2008) 3731, C. Da Via and S. Watts, Nucl. Instr. Meth. A 603 (2009) 318.
4. P. Bussey, FPTrack Programme, http://ppewww.physics.gla.ac.uk/ bussey/FPTRACK.
5. F. Schmidt, Mad-X User's Guide, CERN 2005, http://mad.web.cern.ch/mad.
6. LHC Optics Web Home, http://cern.ch/lhcoptics.
7. W. H. Press, Numerical Recipes, 3rd edition, Cambridge Univ. Press, 2007.
8. T. Sjostrand, P. Eden, C. Friberg, L. Lonnblad, G. Miu, S. Mrenna and E. Norrbin, Computer Phys. Commun. 135 (2001) 238.
9. N. Ohuchi et al., Proc. of EPAC 2002, Paris, France, 2002, p. 2418, E. Todesca, Proc. of LHC Project Workshop – Chamonix XIII, Chamonix, France, 2004, p. 138, O. Bruning et al., Proc. of LHC Project Workshop – Chamonix XIII, Chamonix, France, 2004, p. 178, N. Sammut et al., Proc. of EPAC 2008, Genoa, Italy, 2008, p. 2479, N. Sammut et al., Proc. of EPAC 2008, Genoa, Italy, 2008, p. 2482.
10. M. G. Albrow and A. Rostovtsev, FERMILAB-PUB-00-173 and hep-ph/0009336.